



# Thermally responsive ionic transport system reinforced by aligned functional carbon nanotubes backbone

Lejian Yu<sup>a</sup>, Miao Wang<sup>b,\*</sup>, Xipeng Li<sup>a</sup>, Xu Hou<sup>a,c,d,\*\*</sup>

<sup>a</sup> State Key Laboratory of Physical Chemistry of Solid Surfaces, College of Chemistry and Chemical Engineering, Xiamen University, Xiamen 361005, China

<sup>b</sup> The Higher Educational Key Laboratory for Biomedical Engineering of Fujian Province, Research Center of Biomedical Engineering of Xiamen, Department of Biomaterials, College of Materials, Xiamen University, Xiamen 361005, China

<sup>c</sup> Research Institute for Biomimetics and Soft Matter, Fujian Provincial Key Laboratory for Soft Functional Materials Research, Jiujiang Research Institute, College of Physical Science and Technology, Xiamen University, Xiamen 361005, China

<sup>d</sup> Innovation Laboratory for Sciences and Technologies of Energy Materials of Fujian Province (IKKEM), Xiamen 361005, China

## ARTICLE INFO

### Article history:

Received 1 July 2022

Revised 21 July 2022

Accepted 24 August 2022

Available online 27 August 2022

### Keywords:

Carbon nanotubes arrays

Ion transport system

Interstitial channels

Thermo-controlled

Osmotic energy

## ABSTRACT

Ion transport plays an important role in energy conversion, biosensors, and a variety of biological processes. Carbon nanotubes, especially for the carbon nanotubes arrays with controlled vertically aligned structures, have displayed great potential as a promising material for regulating ion transport behaviors in the applications of the nanofluidic devices and osmotic energy conversion. Herein, we demonstrate the thermo-controlled ion transport system through the vertically aligned multiwall carbon nanotubes arrays membrane modified by the thermo-responsive hydrogel in a simple and reliable way. The functional carbon nanotubes backbone with the inherent surface charge and interstitial channels structure renders the system improved ion transport behaviors and well controlled switching property by thermo. Based on the integrated properties, the energy output from osmotic power in this system could be regulated by the reversible temperature switches. Moreover, it can realize a higher osmotic energy conversion property regulated by the thermos, which may extend the practical application in the future. The system that combines intelligent response with controlled ion transport behaviors and potential osmotic energy utilizations presents a valuable paradigm for the use of carbon nanotubes and hydrogel composite materials and provides a promising way for applications of nanofluidic devices.

© 2023 Published by Elsevier B.V. on behalf of Chinese Chemical Society and Institute of Materia Medica, Chinese Academy of Medical Sciences.

Ion transport in biological channels is the foundation of various physiological functions in life processes, and there has been considerable progress in developing artificial ion channels since its beginning [1–3]. Ion transport in the confined channels, is distinguished from the bulk and exhibits unique effects, which could be applied to various fields, including sensors [4], nanofluidic iontronics [5], aqueous battery [6], desalination [7], and osmotic energy conversion [8,9], *etc.* In terms of the ion transport behaviors, it can be regulated through a chemical modification of channels with corresponding responsive molecules [10], including the stimuli of magnet [11], temperature [12], voltage [13], pH [14], stress [15], *etc.* Among various stimulus-responsive functions, the temperature-responsive ion channels modified by the poly (*N*-isopropyl acry-

lamide) (denote it as PNIPAAm) hydrogel or molecular brushes are one of the most discussed.

Carbon nanotubes (CNTs) are considered as one of the excellent thermal interface materials [16,17] with the one-dimensional graphitic nanochannel structure [18], outstanding thermal and electrical conductivity [16], and desirable mechanical stability [18], which are of particular interest as the backbone materials for fabricating membranes [19,20]. The vertically aligned carbon nanotubes arrays (CNTA) consist of the amounts of CNTs standing perpendicular to a substrate [21], and the CNTA-based membrane has been considered as a promising material for efficient ion transport owing to its high aspect ratio and almost defect-free structure [22,23]. Utilization of CNTs as ion channels is being extensively studied because of many applications are developed in bioengineering fields [24,25], energy harvesting [26] and chemical separation [23].

Hydrogel is of inherent three-dimensional channel structure, meanwhile possessing facile fabrication, excellent electrical conductivity and various environmental responsiveness [27], which enhances the ions shuttling, leading to a high conductance

\* Corresponding author.

\*\* Corresponding author at: State Key Laboratory of Physical Chemistry of Solid Surfaces, College of Chemistry and Chemical Engineering, Xiamen University, Xiamen 361005, China.

E-mail addresses: [miaowang@xmu.edu.cn](mailto:miaowang@xmu.edu.cn) (M. Wang), [houx@xmu.edu.cn](mailto:houx@xmu.edu.cn) (X. Hou).

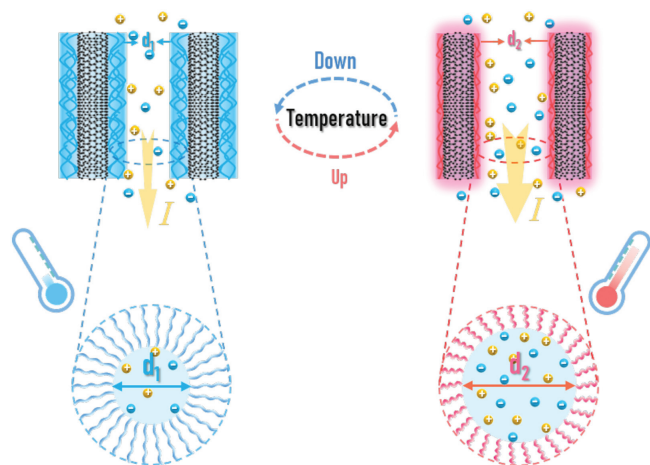


**Fig. 1.** The scheme of the thermo-controlled CPCM membrane system with the changeable effective channels size. The as-prepared CPCM membrane is responsive to the thermal stimulus and exhibits reversible switching behavior triggered by the structural transition of the modified PNIPAAm hydrogel between swollen state (the light blue area, below the LCST) and collapsed state (the light red area, above the LCST). This system can be integrated with the remarkable thermal conductance property (the luminous red area), which shows the difference of the ionic permeability. The  $d_1$  and  $d_2$  are the CPCM membrane effective channels size in low and high temperature, respectively. The yellow arrow represents the ion current. The blue balls and yellow balls denote the anion and cation, respectively.

[14] and have been explored in constructing the flexible electronic devices [28]. For instance, in nature, in order to defend against foreign aggression, the electric eels can generate a high instantaneous voltage from ion gradients, contributed by the unique hydrogel electric organs with excellent ion selectivity and low internal resistance [29].

Based on the above-mentioned unique properties of CNTA and hydrogel, thus, the introduction of hydrogel in CNTA backbone with controlled vertically aligned structures may offer a new orientation for composite membranes fabrication. The multifunctional and smart hydrogels with excellent responsiveness to ambient environments [30,31] can efficiently regulate the ion transport behaviors, and it can be well applied in the various fields, such as wearable electronic [32,33], etc. However, the property of the CNTA composite hydrogel in ion transport system has been rarely explored. Therefore, integrating hydrogels with the unique membrane structure to construct ionic transport system may contribute to the deeper understanding of efficient ion transport for application in artificial systems.

In this work, we demonstrate the construction of thermo-controlled CPCM (CNTA and PNIPAAm composite membrane, denote it as CPCM) membrane system with the changeable effective channels size for realizing an efficient ion transport behavior. The membrane system is constructed by the vertically aligned CNTA, which is embedded with the thermo-sensitive hydrogel. CNTA in this system can provide a high thermal conductivity to facilitate thermal responsiveness, which is reinforced by aligned functional CNTA backbone. Based on the temperature-controlled ion transport behaviors and the improved interfacial ion transport efficiency, the CPCM membrane system presents the promising application in osmotic power harvesting with a controllable and enhanced energy output triggered by the temperature switch. The design concept proposed in this work could be considered as a primal platform of researching the hydrogel functionality of ion channels for ionic transport behaviors regulation, and it may provide new avenues for controllable energy utilization from vast ocean resources in the future.

As revealed in Fig. 1, we have developed the thermo-controlled CPCM membrane system with the changeable effective channels size. The interstitial channels of CPCM membrane among the individual CNTs are embedded with the PNIPAAm hydrogel, which becomes a thermo-controlled ion transport system after graft polymerization. It is generally believed that PNIPAAm hydrogel [34,35] maintains a swollen state and exhibits a thermally responsive transition into a collapsed state below and above the lower critical solution temperature (LCST), respectively. Raising the temperature promotes apparent changes in the conformational state and mechanical property of the PNIPAAm hydrogel (Fig. S1 in Supporting information). In this case, there is an obvious increase of the effective channels size ( $d_2$ ) in the CPCM membrane, which is evidenced as a larger increase in ionic current (right side of the scheme). While for reducing the temperature, an obvious decrease of the effective channel size ( $d_1$ ) appears (left side of the scheme). This reversible system takes the advantage that it provides simultaneously thermally controllable ionic transport properties, and the improved interfacial ion transport efficiency owing to the introduction of PNIPAAm hydrogel and CNTA backbone structure. Also, CNTA, as a thermal interface material with high thermal conductivity, offers the inherent interstitial channels to contribute to thermal conduction of this thermally responsive ionic transport system.

Herein, we directly utilize the CNTA as the original materials, which are subsequently polymerized *in situ* with the PNIPAAm hydrogel to construct the CPCM membrane system, the scheme of fabrication process is provided in Fig. S2 (Supporting information). The optical photographs about macroscopic morphology of the CPCM membrane and CNTA on the left of Fig. 2a show that both their sizes are about  $1.5\text{ cm} \times 1.5\text{ cm}$ . The surface of the CPCM membrane is matte, and the surface of the CNTA is opaque. It is obvious that the FESEM image of microscopic morphology reveals the highly aligned “forest-like” features of CNTA and CPCM membrane, which produces abundant interspace in the form of channels for ionic transportation. Furthermore, we can find that the interspace in the form of channels is wrapped with the porous PNIPAAm hydrogel after polymeric modification in CPCM membrane, for CNTA, we only find amounts of CNTs (right corner of Fig. 2a). Meanwhile, the internal channel of individual CNTs are not mainly the passageway for ionic transportation due to the closed ends of them (Fig. S3 in Supporting information) and they are less than the size of the gap. As shown in Fig. 2b, statistical analysis indicates that the mean size of the interstitial channels of CPCM membrane after polymeric modification is about 200–300 nm. Fig. 2c shows the FTIR spectra of the pristine CNTA (black line), pure hydrogel (blue line) and CPCM membrane (red line), respectively. The FTIR spectra demonstrate that the characteristic vibration peaks attributed to CNTs ( $2000\sim 2200\text{ cm}^{-1}$ ) and PNIPAAm hydrogel with the C-N stretching vibration ( $\sim 1500\text{ cm}^{-1}$ ), C=O stretching vibration ( $\sim 1650\text{ cm}^{-1}$ ) and O-H, N-H stretching vibration characteristic peaks ( $3000\sim 3700\text{ cm}^{-1}$ ) are existed in the CPCM membrane after PNIPAAm hydrogel polymeric modification. Furthermore, the energy dispersive X-ray spectroscopy (EDS) mapping analysis exhibit that the elements of C, O, N are distributed in the CPCM membrane from top view and side view (Fig. S4 in Supporting information), indicating that the hydrogel functionalization with CNTA in this system is available.

The measurement equipment on the transmembrane temperature-controlled ionic transportation behaviors is settled in a two-electrode system. As displayed in Fig. 3a, the homemade device consists of the thermometers two quadrate polymethyl methacrylate (PMMA) containers with a corresponding inlet and an outlet (Fig. S5 in Supporting information). It is noteworthy that this device is improved by circulator bath connected with the heating-cooling cycle water device in both sides. Furthermore, to ensure the permeability of ions, micro holes are punched in

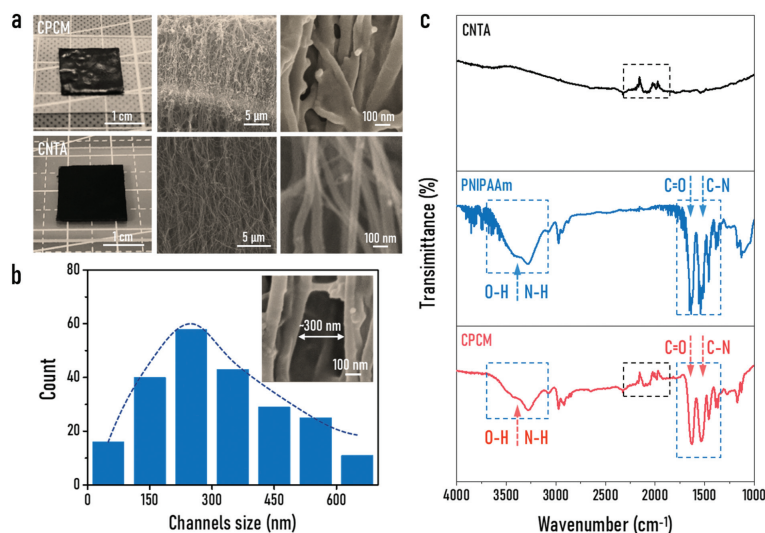


**Fig. 2.** Structural and chemical characterizations. (a) Optical images and FESEM images at high magnifications of CPCM membrane and CNTA, respectively. (b) Statistic channels size distribution of the gap between CNTs for CPCM membrane analyzed from the numerous FESEM images. The inset manifests the FESEM images at high magnifications, indicating the interspace among the CPCM membrane, scale bar: 100 nm. (c) FTIR spectra of the CNTA, PNIPAAm hydrogel and the CPCM membrane.

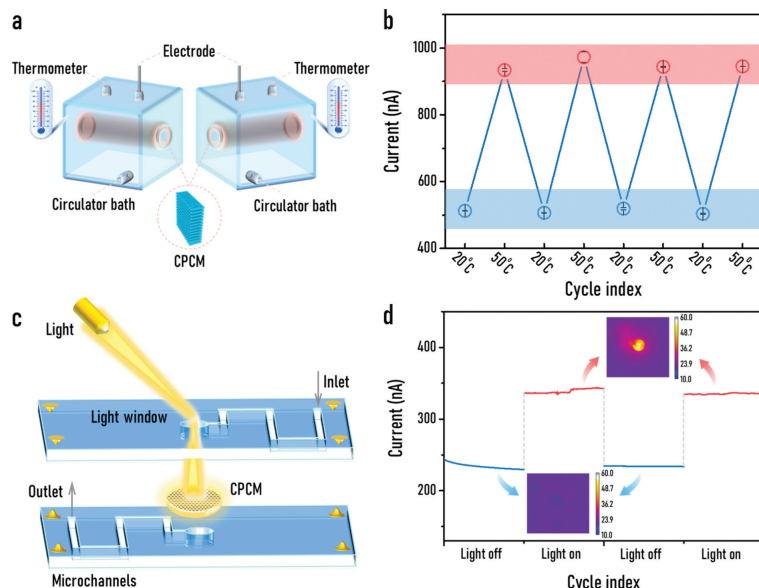


**Fig. 3.** Thermo-controlled behaviors of CPCM membrane system. (a) Schematic of the homemade experimental setup for measuring the temperature-controlled ion transport behaviors, it contains the CPCM membrane, a two-electrode system, the circulator bath system, and the thermometers. (b) Cyclability of CPCM membrane for ion transport through alternately temperature of 20 °C and 50 °C at +1 V in 0.1 mmol/L KCl solution. (c) Schematic structure of the homemade photothermal-regulated microfluidic device, the diameter of light window is 6 mm, and the width of microchannels of the device is 2 mm. (d) Current evolutions at +1 V and the corresponding infrared thermal images for the light stimuli applied on the CPCM membrane.

both containers on the sides facing the membrane test area. As shown in Fig. 3b, the ionic current switching between the low temperature (20 °C) and high temperature (50 °C) states could be reversibly repeated for several cycles. By changing the temperature, the switching response current changes from 500 nA to ~950 nA at +1 V, indicating the CPCM membrane system can be controlled through the thermo change. Besides that, ion transport efficiency of CPCM membrane can be enhanced under high temperature owing to the excellent thermal conductivity and the increase of the effective channels size in hydrogel functionalized CPCM membrane (Fig. S6 in Supporting information). This result implies that the CPCM membrane still remains its deformability (Fig. S7 in Supporting information), even after cyclic varied temperature, and the hydrogel layer in the channels wall of CPCM membrane plays a crucial role in modulating the switching

current, which is conducive to facilitating the interfacial ion transport (Fig. S8 in Supporting information). In the meanwhile, the corresponding infrared thermal curve for CPCM membrane also indicates its exceptional thermal enhancement property owing to the structural characteristics of CNTA backbone, and it offers the fast thermally responsive ionic transport behaviors reinforced by the CNTA backbone (Fig. S9 in Supporting information). The electrolyte concentration (Fig. S10a in Supporting information), electric potential (Fig. S10b in Supporting information), and ion species with the different valence (Fig. S11 in Supporting information) also have an influence on the transmembrane ionic transportation. As the concentration decreases, the measured ionic conductance gradually deviates from the bulk value (red line) at 0.1 mol/L (Fig. S12 in Supporting information), indicating that the transmembrane ionic transport process is also related to the

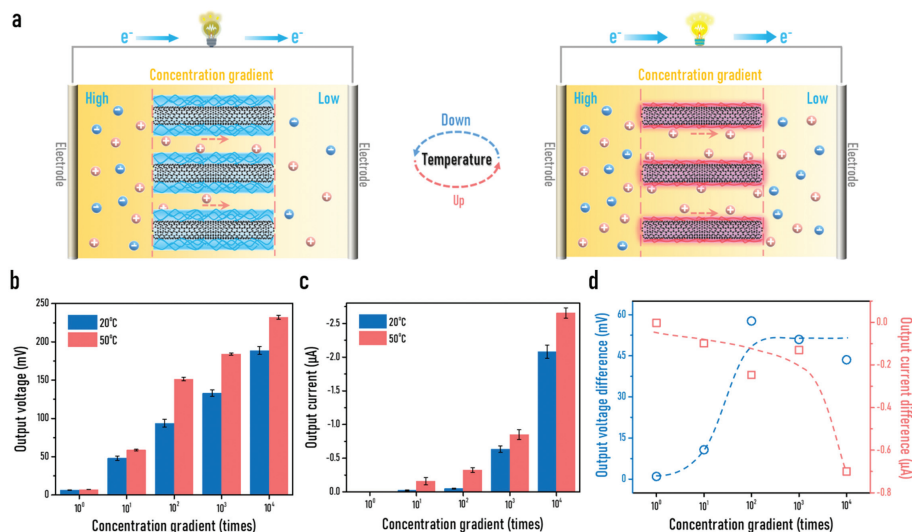


**Fig. 4.** Thermo-controlled CPCM membrane system for enhanced osmotic energy output. (a) The scheme of the thermo-controlled ion transport behaviors for the enhanced osmotic energy output system based on CPCM membrane, the gradual yellow areas represent the concentration gradient. (b) The output voltage with the concentration gradients at different temperatures of 20 °C and 50 °C. (c) The output current with the concentration gradients at different temperatures of 20 °C and 50 °C. (d) The difference value curves of the obtained output voltage and output current from (b) and (c) versus the concentration gradients.

surface charge. Meanwhile, the measured Zeta potentials of the CPCM membrane at various concentrations suggest a negatively charged surface (Fig. S13 in Supporting information).

As previous studies have shown, CNTA exhibits an outstanding thermal conductance [36,37] on account of its unique structure and properties, which is a potent candidate for the photothermal material since it generates significant amounts of heat upon excitation with the light. Inspired by that, a homemade photothermal-regulated microfluidic device is designed. As exhibited in Fig. 3c, the CPCM membrane is assembled between the two silicone slices and two separate chambers with designed channels (Fig. S14 in Supporting information), and the light window on the top of the device is reserved for light regulation. Top and bottom chambers with designed channels could be injected with the solution *via* individual inlet/outlet. To further probe the entire light-controlled ion transport behaviors, we measure the current evolutions at +1 V of the 0.1 mmol/L KCl solution through the CPCM membrane system under the switches of light irradiation cycles (Fig. 3d). The light-controlled ion transport behavior exhibits good current switching performance with systematically varied light on/off. Meanwhile, this behavior is monitored by the real-time temperature of the CPCM membrane using the infrared thermal images (the inset in Fig. 3d). This can be attributed to the photothermal property of CPCM membrane system under the light, in which the effective channel size changes with the structural transformation of the PNIPAAm hydrogel, revealing that the ionic transportation behavior can also be tuned in virtue of light (Fig. S15 in Supporting information).

Inspired by the excellent ion transport behaviors of the thermo-controlled CPCM membrane system, we further develop CPCM membrane into an energy conversion device, which can be conducive to efficiently capturing osmotic energy from the concentration gradient. Here, KCl is selected on account of the comparable diffusion coefficients of K<sup>+</sup> cation ( $\sim 1.96 \times 10^9$  m<sup>2</sup>/s) and Cl<sup>-</sup> anion ( $\sim 2.03 \times 10^9$  m<sup>2</sup>/s), which permits the minimization of the liquid junction potentials [38]. In Fig. 4a, concentration gradient across the channels of CPCM membrane is illustrated, containing two Ag/AgCl electrodes employed to connect the external circuit for energy output, and the solution with different concentrations at both ends. The PNIPAAm hydrogel of CPCM membrane undergoes thermally responsive formation of intermolecular hydrogen-

bonding between PNIPAAm chains and water molecules, and intramolecular hydrogen-bonding between C=O and N-H groups at 20 °C and 50 °C [32], and the PNIPAAm hydrogel layer can improve the interfacial ion transport efficiency. In this energy conversion system, there is an increase of the effective channels size, and the ionic current increase coming from the conductivity changes due to temperature variations and improved interfacial ion transport efficiency, which is beneficial for the osmotic energy output. As the CPCM membrane is negatively charged in the KCl solution, under the concentration gradient, a diffusion current is induced due to the net K<sup>+</sup> flux across the channels, leading to the diffusion potential and diffusion current output in the external circuit [39].

To evaluate the osmotic energy conversion performance, the corresponding open-circuit voltage and short-circuit current measurements under different concentration gradients are conducted. The KCl concentration on low concentration side is maintained at 0.1 mmol/L, and the relative high concentrations side is varied from 0.1 mmol/L to 1 mol/L. In Fig. 4b, we can find that the output voltage is boosted by the high temperature (50 °C) under various concentration gradients (Fig. S16 in Supporting information), and the output current in Fig. 4c also shows an upward tendency in the same condition (Fig. S17 in Supporting information), showing the maximum output voltage ( $\sim 230$  mV) and output current ( $\sim 2.65$  μA) at 50 °C under 10<sup>4</sup> times concentration gradient. Besides that, it shows a sustained and stable energy output both in low and high temperature under a series of concentration gradients. Fig. 4d summarizes the difference value of the output voltage and current at the temperature difference under a series of concentration gradients. The maximum increment for output voltage and current at 10<sup>4</sup> times concentration gradient can reach  $\sim 45$  mV and  $\sim 0.7$  μA, respectively. It reveals that the introduction of PNIPAAm functional hydrogel in this system at high temperature leads to an enhanced conductivity state, which contributes to facilitate the ion transport through the channels of CPCM membrane with an enhancement in the output voltage and current.

In summary, we demonstrate the CPCM membrane system with the temperature-controlled ion transport behaviors and the improved interfacial ion transport efficiency, which can be applied in osmotic power harvesting with a controllable and enhanced energy output. This membrane system is constructed through *in situ* polymerization method with temperature-responsive hydrogel

onto vertically aligned CNTA. By means of the outstanding thermal conductivity and inherent interstitial channels, the thermally responsive ionic transport system can be reinforced by the CNTA backbone structure, and the temperature-controlled ion transport behaviors can be improved under the thermal environment. Meanwhile, the hydrogel is employed on the channels to boost hydrophilicity and facilitate the ion transport interfacial efficiency. Besides that, such a membrane system based on the vertically aligned CNTA with hydrogel can increase the osmotic energy conversion with a maximum enhanced output voltage of  $\sim 60$  mV and current of  $\sim 0.7$   $\mu$ A, which offers a way of the potential application on the osmotic power generation through membrane interfacial design. The system exploits the inherent interstitial channels of CNTA and responsive hydrogel to improve the interfacial properties of ion channels, providing a basic example which may potentially spark further efforts for the application of investigating the physical processes of biological systems, sensing, membrane separation, drug release and energy conversion, etc.

#### Declaration of competing interest

The authors declare that they have no known competing financial interests or personal relationships that could have appeared to influence the work reported in this paper.

#### Acknowledgments

This study is supported by the National Natural Science Foundation of China (Nos. 21975209, 52025132 and 21621091) and the National Key R&D Program of China (No. 2018YFA0209500). The authors thank Liting Pan for beneficial discussion.

#### Supplementary materials

Supplementary material associated with this article can be found, in the online version, at doi:10.1016/j.ccl.2022.107785.

#### References

- [1] Y. Chen, Z. Zhu, Y. Tian, et al., Exploration 1 (2021) 20210101.
- [2] Z. Zhu, D. Wang, Y. Tian, et al., J. Am. Chem. Soc. 141 (2019) 8658–8669.
- [3] M. Wang, Y. Hou, L. Yu, et al., Nano Lett. 20 (2020) 6937–6946.
- [4] K. Xiao, C. Wan, L. Jiang, et al., Adv. Mater. 32 (2020) e2000218.
- [5] Y. Hou, X. Hou, Science 373 (2021) 628–629.
- [6] C. Yang, J. Chen, X. Ji, et al., Nature 569 (2019) 245–250.
- [7] X. Zhou, Z. Wang, R. Epsztein, et al., Sci. Adv. 6 (2020) eabd9045.
- [8] Z. Zhang, L. Wen, L. Jiang, Nat. Rev. Mater. 6 (2021) 622–639.
- [9] W. Chen, T. Dong, Y. Xiang, et al., Adv. Mater. 34 (2022) e2108410.
- [10] X. Hou, Adv. Mater. 28 (2016) 7049–7064.
- [11] C. Wang, D. Wang, W. Miao, et al., ACS Nano 14 (2020) 12614–12620.
- [12] X. Zuo, C. Zhu, W. Xian, et al., Angew. Chem. Int. Ed. 61 (2022) e202116910.
- [13] Y. Zhou, J. Hao, J. Zhou, et al., Matter 5 (2022) 281–290.
- [14] K. Zhan, Z. Li, J. Chen, et al., Nano Today 33 (2020) 100868.
- [15] M. Wang, H. Meng, D. Wang, et al., Adv. Mater. 31 (2019) e1805130.
- [16] L. Ping, P.X. Hou, C. Liu, et al., APL Mater. 7 (2019) 020902.
- [17] W. He, L. Zhou, M. Wang, et al., Sci. Bull. 66 (2021) 1472–1483.
- [18] H. Dai, Acc. Chem. Res. 35 (2002) 1035–1044.
- [19] J.H. Lee, H.S. Kim, E.T. Yun, et al., Membranes 10 (2020) 273.
- [20] Y. Hou, Q. Wang, S. Wang, et al., Chin. Chem. Lett. 33 (2022) 2155–2158.
- [21] M. Wang, T. Li, Y. Yao, et al., J. Am. Chem. Soc. 136 (2014) 18156–18162.
- [22] S. Zhou, J. Sheng, Z. Yang, et al., J. Mater. Chem. A 6 (2018) 8763–8771.
- [23] M. Barrejón, M. Prato, Adv. Mater. Interfaces 9 (2021) 2101260.
- [24] L. Ye, H. Ji, J. Liu, et al., Adv. Mater. 33 (2021) 2102981.
- [25] Y. Fan, Y. Hou, M. Wang, et al., Mater. Adv. 3 (2022) 3070–3088.
- [26] L. Zhang, F. Liu, S. Yang, et al., Adv. Membr. 2 (2022) 100026.
- [27] Y. Guo, J. Bae, Z. Fang, et al., Chem. Rev. 120 (2020) 7642–7707.
- [28] H. Zhang, J. Guo, Y. Wang, et al., Adv. Sci. 8 (2021) e2102156.
- [29] T.B.H. Schroeder, A. Guha, A. Lamoureux, et al., Nature 552 (2017) 214–218.
- [30] A.A. Adewunmi, S. Ismail, A.S. Sultan, J. Inorg. Organomet. Polym. Mater. 26 (2016) 717–737.
- [31] C. Lei, Z. Xie, K. Wu, et al., Adv. Mater. 33 (2021) e2103495.
- [32] Y. Yu, J. Guo, B. Ma, et al., Sci. Bull. 65 (2020) 1752–1759.
- [33] Y. Yu, J. Guo, L. Sun, et al., Research 2019 (2019) 6906275.
- [34] J. Liu, L. Jiang, S. He, et al., Chem. Eng. J. 433 (2022) 133496.
- [35] B. Chen, M. Zhang, Y. Hou, et al., Innovation 3 (2022) 100231.
- [36] K.H. Baloch, N. Voskanian, M. Bronsgeest, et al., Nat. Nanotechnol. 7 (2012) 316–319.
- [37] C. Boo, M. Elimelech, Nat. Nanotechnol. 12 (2017) 501–503.
- [38] Z. Zhang, L. He, C. Zhu, et al., Nat. Commun. 11 (2020) 875.
- [39] W. Chen, Y. Xiang, X. Kong, et al., Giant 10 (2022) 100094.